American Physiological Society | AMERICAN JOURNAL OF PHYSIOLOGY Renal Physiology

PUBLISHED ARTICLE
ARCHIVES
SUBSCRIPTIONS
SUBMISSIONS
CONTACT US

Am J Physiol Renal Physiol. 2013 Sep 1; 305(5): F691–F700. PMCID: PMC3761209
Published online 2013 Jun 26. doi: 10.1152/ajprenal.00028.2013

The antioxidant silybin prevents high glucose-induced oxidative stress and podocyte injury in vitro and in vivo

Khaled Khazim,[2,3] Yves Gorin,[2] Rita Cassia Cavaglieri,[2] Hanna E. Abboud,[1,2] and Paolo Fanti[1,2]

[1]South Texas Veterans Health Care System, Audie L. Murphy Memorial Hospital Division, San Antonio, Texas;
[2]Department of Medicine, University of Texas Health Science Center, San Antonio, Texas; and
[3]Nephrology and Hypertension Unit, Western Galilee Hospital, Nahariya, Israel
Corresponding author.
Address for reprint requests and other correspondence: P. Fanti, Univ. of Texas Health Science Center, Dept. of Medicine, Division of Nephrology MC 7882, 7703 Floyd Curl Drive, San Antonio, TX 78229-3900 (e-mail: fanti@uthscsa.edu).

Received 2013 Jan 15; Accepted 2013 Jun 25.

Abstract

Podocyte injury, a major contributor to the pathogenesis of diabetic nephropathy, is caused at least in part by the excessive generation of reactive oxygen species (ROS). Overproduction of superoxide by the NADPH oxidase isoform Nox4 plays an important role in podocyte injury. The plant extract silymarin is attributed antioxidant and antiproteinuric effects in humans and in animal models of diabetic nephropathy. We investigated the effect of silybin, the active constituent of silymarin, in cultures of mouse podocytes and in the OVE26 mouse, a model of type 1 diabetes mellitus and diabetic nephropathy. Exposure of podocytes to high glucose (HG) increased 60% the intracellular superoxide production, 90% the NADPH oxidase activity, 100% the Nox4 expression, and 150% the number of apoptotic cells, effects that were completely blocked by 10 μM silybin. These in vitro observations were confirmed by similar in vivo findings. The kidney cortex of vehicle-treated control OVE26 mice displayed greater Nox4 expression and twice as much superoxide production than cortex of silybin-treated mice. The glomeruli of control OVE26 mice displayed 35% podocyte drop out that was not present in the silybin-treated mice. Finally, the OVE26 mice experienced 54% more pronounced albuminuria than the silybin-treated animals. In conclusion, this study demonstrates a protective effect of silybin against HG-induced podocyte injury and extends this finding to an animal model of diabetic nephropathy.

Keywords: albuminuria, apoptosis, diabetic nephropathy, NADPH oxidase, phytochemicals

THE PODOCYTES ARE TERMINALLY differentiated and highly specialized glomerular visceral epithelial cells that, along with the endothelial cell layer and the glomerular basement membrane (GBM), participate in the formation of the glomerular filtration barrier and in the prevention of urinary protein loss (26). Podocyte injury leads to proteinuria and is considered a major contributor to the initiation and progression of both diabetic and nondiabetic glomerular disease (35, 46). Patients with early type 1 and type 2 diabetes mellitus experience loss of podocytes (41, 48) and show correlation between the rate of albumin excretion and the drop in podocyte number (34, 59). In addition, mouse models of both type 1 and 2 diabetes demonstrate a sharp increase in podocyte apoptosis (50) and reduction in podocyte/slit diaphragm protein expression shortly after the onset of hyperglycemia and proteinuria (34).

Oxidative damage from both free radical and nonradical oxygen species (18) contributes to the pathogenesis of diabetic complications including onset and progression of diabetic kidney disease (58). Both experimental and clinical studies have documented a link among hyperglycemia, oxidative stress, and diabetic nephropathy (6, 40). More recently, reactive oxygen species (ROS)-mediated effects of HG have been implicated in podocyte injury and apoptosis (13, 16). In this context, the NADPH oxidase isoform Nox4 has emerged as one of the most important sources of ROS in the kidney (22, 45).

The flavonolignan silybin also known as silibinin is the most abundant (50–70%) and the most active component of silymarin (31), an extract from the plant milk thistle (*silybum marianum*, *Asteraceae* family). Silymarin exerts hepatoprotective effects and has been used for centuries as an herbal remedy for liver disease (21). In vitro studies showed

that silymarin has both antioxidant and anti-inflammatory effects (9), including inhibition of superoxide production in Küpffer cells (13). In addition, silybin prevents hydrogen peroxide-induced apoptosis of endothelial cells (56). Silymarin also appears to reduce proteinuria in a rat model of streptozotocin-induced diabetes and in patients with type 2 diabetes (17, 55). The mechanisms by which silymarin exerts these effects are unknown.

These observations led us to formulate the hypothesis that silybin through its antioxidant effects reduces proteinuria by direct effects on the podocyte. The studies described in this study explore the effect of silybin on podocyte injury in vitro in cultured podocytes and in vivo in a mouse model of type 1 diabetes.

MATERIALS AND METHODS

Materials

Chemical reagents were purchased from Sigma-Aldrich (St. Louis, MO) unless stated otherwise. Silybin stock solution (20 mM final concentration) was prepared in dimethyl sulfoxide (DMSO); for the in vitro experiments, the stock was directly dissolved in the culture media. For the in vivo experiments, silybin was first diluted 1:10 with DMSO and then 4/46/46 (vol/vol/vol) with propylene glycol and normal saline to a final concentration of 80 μM.

Cell Culture

Conditionally immortalized mouse podocytes were grown to near confluence and reseeded three times under growth-permissive conditions (33°C) in flasks coated with type I collagen in a humidified chamber with 5% CO_2. Growth media consisted of RPMI 1640 with 10% fetal bovine serum, 100 U/ml of penicillin/streptomycin, and 5 mM D-glucose (NG). The medium was supplemented with 50 U/ml of mouse interferon-γ (INF-γ) during the first passage and then 10 U/ml INF-γ in the second and third passage. Cell differentiation was then induced by subculturing the cells under nonpermissive conditions (37°C) in serum-containing medium without INF-γ for 10–14 days (46). Cells were serum starved for 24 h before the experiment with RPMI 1640 containing NG and 0.2% BSA. The experiment consisted of overnight pretreatment of the cells with silybin at a final concentration of 10 μM or with vehicle. Cells were then exposed to NG or 25 mM D-glucose (HG) with or without silybin for 24 h.

Animal Models

OVE26 mice (FVB background; The Jackson Laboratory, Bar Harbor, ME) were used as a model of type 1 diabetes mellitus and FVB mice as nondiabetic control animals. At 6 wk of age, mice were started on an animal protein-based diet (Teklad irradiated global soy protein-free extruded rodent diet-2920X) and animals were provided food and water ad libitum; at 10 wk they were started on 100 mg/kg silybin or vehicle given intraperitoneally for 6 wk (6 animals in each group). Urine collections were done in metabolic cages, and the urine albumin-to-creatinine ratio was measured using commercial kits for mouse albumin (Bethyl Laboratories, Montgomery, TX) and creatinine (Enzo Life Science, Farmingdale, NY). Blood glucose was measured using a glucose meter with detection range 10–600 mg/dl (Contour; Bayer Healthcare, Tarrytown, NY). The animals were killed by exsanguination under anesthesia. The cortex of one kidney was flash-frozen in liquid nitrogen for microscopy and image analysis, while the contralateral organ was fixed in 10% formalin for 24 h and then embedded in paraffin for immunohistochemistry. The Institutional Animal Care and Use Committee of the University of Texas Health Science Center San Antonio approved the protocol.

NADPH Oxidase Activity

NADPH oxidase activity was measured in cultured podocytes using lucigenin-enhanced chemiluminescence as described previously (23). Cells were washed with ice-cold phosphate-buffered saline and scraped from the plate in lysis buffer (20 mM KH_2PO_4 pH 7.0, containing protease inhibitor cocktail; Roche Diagnostics, Indianapolis, IN). The material was homogenized (100 strokes) using an ice-cold Dounce homogenizer. To start the assay, 25 μg of homogenates were added to 50 mM phosphate buffer (pH 7.0) containing 150 mM sucrose, 5 μM lucigenin, and 100 μM NADPH. Photon emission expressed as relative light units was measured every 30 s for 5 min by luminometry. Superoxide production was expressed as relative light units per minutes per milligrams of protein. Protein content was measured using Bio-Rad Protein Assay Reagent (Bio-Rad laboratories, Hercules, CA).

Detection of Intracellular Superoxide

Intracellular superoxide anion production was measured by analyzing the conversion of the fluorescent probe dihydroethidium (DHE) into dihydroxyethidium (2-OH-E^+) adopting an established high-performance liquid

chromatography (HPLC)-based method with minor modifications (29). All buffers were cleared from trace elements by pretreatment with Chelex and conditioning with 100 μM diethylene triamine pentaacetic acid (DTPA). Cultured podocytes were plated in 60-mm dishes, treated as per protocol, washed two times with Hanks'/DTPA, and finally incubated at 37° C, 5% CO_2 for 30 min with 50 μM DHE in Hanks'/DTPA. The incubation was stopped by transferring the cultures to an ice bath and by washing with cold PBS/DTPA, followed by the addition of acetonitrile (500 μl per dish) and immediate cell harvest by scraping. After centrifugation of the lysates at 12,000 *g* for 10 min (4°C), the supernatants were dried using a speed-vac system. Pellets were stored at −20°C in the dark for not >4 wk. For HLPC analysis, the dried samples were resuspended in 120 μl PBS/DTPA, and 100 μl were injected into a HPLC system (LC-2000 plus series; Jasco Analytical instruments, Easton, MD) equipped with a C-18 column (Nucleosil 100–5, Macherey-Nagel, Germany) and with ultraviolet and fluorescence detectors. Elution of analytes was achieved with acetonitrile (*solvent A*) and water with 0.1% trifluoroacetic acid (vol/vol; *solvent B*) as mobile phase, with a flow rate of 0.6 ml/min and with the following *solvent A* gradient: 10% at *time 0* (sample injection) and 60% at *minute 10* (linear increase) and through *minute 20* (isocratic). Elution of 2-OH-E^+ was monitored by fluorescence with emission and excitation wavelengths at 595 and 510 nm, respectively, while elution of DHE was monitored by ultraviolet using 370-nm wavelength. The retention times for DHE and 2-OH-E^+ were 12.5–13.5 and 16–17 min, respectively. The eluate mass was quantified by comparing the peak area of the unknown samples with those of standards 2-OH-E^+ (Noxygen, Denzlingen, Germany). Superoxide was also measured in finely minced kidney cortex from the experimental animals (see above). The minced tissue was washed three times with PBS/DTPA followed by a 30-min incubation with 100 μM DHE in 500 μl PBS/DTPA at 37°C in the dark. The tissue was then washed with PBS/DTPA, flash frozen in liquid nitrogen, homogenized, and resuspended in 500 μl acetonitrile, lysed by sonication, and centrifuged at 12,000 *g* for 10 min at 4°C. The supernatants were dried using a speed-vac system and analyzed by HPLC as described above.

Detection of Intracellular ROS by Immunofluorescence

Intracellular superoxide production was measured using the cell-permeable dye DHE (Invitrogen, Grand Island, NY), which binds to nuclear DNA when oxidized by superoxide and emits red fluorescence. Cells were plated in a four-well Chambered Coverglass (cat no. 155383; Lab-Tek, Hatfield, PA), treated as per protocol, washed twice with phenol-free Hanks' buffer, and incubated with 10 μM DHE in a light-protected humidified chamber at 37°C for 15 min. After incubation, the cells were washed twice with Hanks' buffer and immediately imaged by a laser-scanning confocal microscopy with appropriate filters (excitation 520 nm and emission 610 nm) (24). Mean fluorescence intensity of the image was measured with ImageJ software for quantification.

Western Immunoblotting

Podocytes were grown in 100-mm dishes and treated as per protocol. The cells were washed 3 times with PBS then lysed with RIPA buffer (20 mmol/l Tris·HCl pH 7.5, 150 mM NaCl, 5 mM EDTA, 1 mM Na_3VO_4, and 1 mM phenylmethylsulfonyl fluoride) and protease cocktail inhibitors (Roche Diagnostics) at 4°C for 30 min. The cell lysates were centrifuged at 10,000 *g* for 30 min at 4°C. Protein was determined in the cleared supernatant using the Bio-Rad method. For immunoblotting, 20–40 μg of protein were separated by 10% SDS-PAGE and transferred to poyvinylidene difluoride membranes. Blots were incubated overnight with rabbit polyclonal anti-Nox4 IgG or anti-Nox1/Mox1 IgG (1:250 and 1:500, respectively; Santa Cruz Biotechnology, Dallas, TX). The primary antibody was detected using horseradish-conjugated IgG (1:10.000). Bands were visualized by enhanced chemiluminescence. Densitometric analysis was performed using ImageJ imaging and processing software (43).

Cellular DNA Fragmentation and Apoptosis Assays

Cultured cell lysates were tested for DNA fragmentation using a commercial ELISA that detects bromodeoxyuridine-labeled DNA fragments (Roche Diagnostics). Cell apoptosis was also imaged with the Hoechst nuclear dye following the manufacturer's protocol (33258; Sigma). After fixation with 1.5% formalin in PBS for 20 min at room temperature (RT), cells were bathed with cold methanol (−20 °C) and incubated for 20 min at RT for permeabilization, washed with PBS, incubated with Hoechst stain (0.12 μg/ml; Thermo Scientific, Rockford, IL) for 15 min at RT, washed with PBS, and finally analyzed with a fluorescence microscope with 340- and 460-nm excitation and emission wavelengths.

Immunohistochemistry

Analysis of Nox4 and Wilm's tumor 1. For analysis of Nox4 expression, kidney sections or cell monolayers were fixed in 10% formalin, embedded in paraffin, and subjected to microwave irradiation at 2,400 W for 6 min in citrate buffer to enhance antigen retrieval. For analysis of Wilm's tumor 1 (WT-1) expression, frozen kidney sections were fixed in acetone for 10 min.

All slides were quenched in 3% hydrogen peroxide for 6 min, washed in TBS, blocked with Sniper blocking buffer (Biocare Medical, Concord, CA) for 20 min, and then incubated with either rabbit polyclonal anti-Nox4 (1:500; no. NB110-58851; Novus Biologicals) or rabbit polyclonal anti-WT-1 (1:400; no. sc192; Santa Cruz Biotechnologies) overnight at 4°C in a humidified chamber. After being rinsed, the slides were incubated with goat anti-rabbit polymer-horseradish peroxidase (Biocare Medical) for 20 min at RT. Immunoreactivity was visualized with 3-3′-diaminobenzidine (Biocare Medical). Negative controls were processed by omitting the incubation with the primary antibody. Sections were photographed using Zeiss Axio Imager A1 (Melville, NY).

Podocyte count. Dual-label immunohistochemistry was used to identify and count podocytes relative to the GBM in 6-μm frozen sections of kidney cortex as previously described (15). Tissue sections were layered on glass slides and stained with a goat anti-synaptopodin antibody (Santa Cruz Biotechnology) followed by Cy3-labeled donkey anti-goat IgG (EMD Millipore, Billerica, MA). To identify the GBM, the sections were then stained with a rabbit antibody directed against collagen type IV (EMD Millipore) followed by FITC-labeled donkey anti-rabbit IgG (EMD Millipore). After being stained and washed, the sections were preserved on coverslips in Prolong gold antifade mounting medium with 4′,6-diamidino-2-phenylindole (Invitrogen) for the fluorescence detection of nuclei. Sections were examined by epifluorescence using excitation and band-pass filters optimal for FITC, Cy3, and 4′,6-diamidino-2-phenylindole. Digital images representing each fluorochrome of random glomeruli were taken using an AX70 Research microscope and a DP70 digital camera (Olympus, Melville, NY). Twenty-five to thirty glomerular cross sections per animal were photographed in each color channel providing a minimum of 75 composite images per experimental group. The images were merged and color balanced using Image-Pro Plus imaging software (Media Cybernetics, Silver Spring, MD). Synaptopodin-positive cells on the outer aspect of the GBM were identified as podocytes and counted. Synaptopodin-negative cells or those in the inner aspect of the GBM were not counted.

Statistical Analysis

Data are expressed as means ± SE. Difference between groups was tested using Student's unpaired *t*-test or one-way ANOVA with Student-Newman-Keuls post hoc comparison, as appropriate. Statistical significance was assessed at the $P \leq 0.05$ level.

RESULTS

In Vitro Studies

Effects of silybin on glucose-induced superoxide generation in cultured mouse podocytes. The effect of silybin on HG-induced intracellular ROS generation in cultured mouse podocytes was tested using DHE fluorescence and confocal microscopy. As shown in Fig. 1*A*, exposure of podocytes to HG resulted in 70% increase of intracellular ROS production, and this increase was completely inhibited by coincubation of the cells with 10 μM silybin. Generation of superoxide was also analyzed by quantifying the production of 2-OH-E^+, the superoxide specific product of DHE, by HPLC. Exposure of the podocytes to HG caused 60% increase in 2-OH-E^+ production, and this effect was abrogated by coincubation with silybin (Fig. 1*B*). Figure 1*C* shows a dose-dependent response to silybin; incubation with 0.1 μM silybin inhibited partially the HG-induced generation of 2-OH-E^+, while 1 and 10 μM silybin resulted in complete inhibition.

Effect of silybin on glucose-induced NADPH oxidase activity in podocytes. Since NADPH oxidases of the Nox family are a major source of superoxide in renal cells, including podocytes, we assessed NADPH oxidase activity in podocytes under the same experimental conditions as above, using the lucigenin-enhanced chemiluminescence assay. The NADPH-dependent superoxide generation increased by 90% after exposure of the cells to HG for 24 h. Treatment with silybin completely suppressed HG-induced increase in NADPH oxidase activity (Fig. 2*A*). Western blot analysis showed that HG-mediated increased expression of Nox4 protein expression is totally inhibited by silybin treatment (Fig. 2*B*). Analysis of Nox1 yielded similar results, although the constitutive and HG-indued expression of this protein was weaker than for Nox4 (Fig. 2*C*).

Effect of silybin on glucose-induced podocytes injury. Apoptotic cell death is one of the manifestations of podocyte injury in the diabetic milieu. Podocytes apoptosis was examined in vitro by two different methods, Hoechst staining and DNA fragmentation (20). As shown by Hoechst staining (Fig. 3*A*), exposure of the podocytes to HG for 24 h resulted in significant podocyte apoptosis compared with NG, while silybin protected against HG-induced podocyte apoptosis. Likewise, silybin completely prevented DNA fragmentation, a measure of podocyte apoptosis induced by HG (Fig. 3*B*).

Studies on a type 1 diabetic mouse model. To validate the findings in cultured immortalized mouse podocyte, we studied the effect of silybin on an established mouse model of type 1 diabetes, the OVE26 mouse. These mice develop morphological and structural changes characteristics of human diabetic nephropathy (63). Three groups of mice were studied: *1*) FVB

control animals, *2*) control diabetic OVE26 animals treated with vehicle, and *3*) OVE26 diabetic mice treated with silybin for 6 wk. Blood glucose levels were 130.4 ± 12.4 mg/dl in the FVB control animals and above the detection limit (600 mg/dl) in the OVE26 diabetic groups, irrespective of treatment with vehicle or silybin.

Effects of silybin on superoxide production in the renal cortex. Superoxide production was measured in kidney cortex using DHE and HPLC. 2-OH-E^+ production was increased in the renal cortex from diabetic mice and silybin treatment significantly reduced the increase of 2-OH-E^+ in OVE26 mice (Fig. 4*A*). In addition, immunohistochemistry of kidney cortex showed increased expression of Nox4 in the OVE26 mice compared with the FVB control mice (Fig. 4*B*). Silybin treatment prevented the increased expression of Nox4 in the OVE26 mice (Fig. 4*B*).

Effects of silybin on the number of resident podocytes. Loss of podocytes in diabetic mice was detected by counting the number of synaptopodin-positive cells in glomeruli (Fig. 5, *A* and *B*). Dual-label immunohistocytochemistry/immunofluorescence was used to identify and count podocytes relative to the GBM stained with collagen IV (Fig. 5*B*). As shown in Fig. 5, *A* and *B*, synaptopodin staining is significantly reduced in type 1 diabetic OVE26 mice compared with FVB mice. Treatment with silybin for 6 wk prevented diabetes-induced podocytes loss (Fig. 5, *A* and *B*). The expression of WT-1 is restricted to podocytes in mature glomeruli (37, 49). Therefore, we also evaluated the number of podocytes in glomeruli using WT-1 staining. The number of the WT-1-positive cells in glomerular sections (20–25 glomeruli per animal, 3 animals per group) was reduced in the diabetic mice, and this effect of diabetes was prevented by treatment with silybin (Fig. 5*C*).

Effect of silybin on albuminuria. The diabetic mice developed severe albuminuria when compared with the nondiabetic mice. Silybin treatment attenuated the albuminuria in the diabetic mice by 54% ($P = 0.06$; Fig. 5*D*).

DISCUSSION

The present study demonstrates a protective effect of the flavonolignan silybin on renal injury and albuminuria in the OVE26 mouse, an animal model of type 1 diabetes. In addition, the study provides in vivo and in vitro evidence demonstrating that the mechanisms by which silybin exerts its renoprotective effect involve inhibition of NADPH oxidase activity and prevention of podocyte apoptosis (Fig. 6).

Consistent with the original description of the OVE26 model, our mice were hyperglycemic shortly after birth and they displayed severe proteinuria and significant loss of podocytes at the age of 16 wk. As a novel observation, we report that treatment with silybin for 6 wk prevented podocyte loss and reduced albuminuria by 54% without affecting blood glucose levels. Albuminuria is the strongest independent clinical predictor of progression to end stage renal disease in diabetic patients (1, 3, 11, 28), and reduction of albuminuria and proteinuria is associated with slower decline in glomerular filtration rate and reduced risk for end stage renal disease (7, 44). Furthermore, glomerular podocyte loss is an early event in the pathogenesis of diabetic nephropathy (48, 60, 61) and murine models of diabetic nephropathy have shown that podocyte apoptosis precedes the onset of albuminuria and mesangial matrix expansion (30). In this context, the ability of silybin to correct both podocyte loss and albuminuria in diabetic nephropathy represents a new and/or additional therapeutic option to the conventional established antiproteinuric treatment strategies. In this study, we did not monitor blood pressure because prior research showed that 16-wk-old OVE26 mice have similar or slightly lower blood pressure than control FVB mice and that OVE26 mice experience an increase in the systolic blood pressure only at 8 mo of age (10, 63).

Of interest is that milk thistle and silymarin, a silybin-enriched milk thistle extract, have recently been reported to increase the renal activity of certain antioxidant enzymes (catalase and glutathione peroxidase) and to protect the kidneys from diabetic damage in streptozotocin-treated rats (55). Treatment with silymarin also reduced albuminuria in type 2 diabetic patients (17). Furthermore, the effect of silybin seems not to be limited to diabetic nephropathy since this flavonoid was shown to prevent glomerular and tubular cell injury and apoptosis in cisplatin- and arsenic-treated rats (5, 19, 42). The present study adds to the existing evidence not only by demonstrating a renoprotective effect of silybin in a new animal model of type 1 diabetes but also by providing strong evidence that prevention of podocyte injury is a major underlying mechanism of this protective effect.

Podocyte injury in diabetes results from oxidative stress mediated primarily by NADPH oxidases of the Nox family (50). Indeed, Nox-dependent ROS generation and specifically the ROS produced by the isoform Nox4 are now recognized as a key effector of renal cell damage, including podocyte injury and depletion that characterize the early stages of diabetic kidney disease. In the present study, we confirm previous observations indicating that Nox4 expression is increased in podocytes exposed to glucose (16, 22, 26, 45). We have previously shown that impairment of Nox4 function with an adenovirus encoding a dominant-negative form of Nox4 significantly inhibits glucose-induced NADPH oxidase activity and

podocyte apoptosis, demonstrating that Nox4 is critical for podocyte injury in the diabetic milieu (15). In our in vitro studies, silybin inhibited HG-induced Nox4 protein upregulation, NADPH oxidase activity, and intracellular superoxide production. This was associated with decreased apoptosis of podocytes exposed to HG. Collectively, these data strongly suggest that silybin may exert its protective actions via inhibition of HG-induced increase in Nox4 expression and the subsequent increase in Nox4-dependent ROS generation. These data offer a plausible mechanistic explanation for the in vivo effects of silybin, which thus appear to be mediated at least partially by inhibition of NADPH oxidase activity and of superoxide anion production with consequent antioxidant and antiapoptotic effects in podocytes. With these experiments, we also confirm that the stimulatory effect of HG on podocytes is not limited to Nox4 but it also affects expression of the Nox1 isoform (15) and we demonstrate that the downregulatory action of silybin involves both Nox4 and Nox1. It is possible that Nox1 may also contribute to podocyte injury in diabetes, although the functional significance of this isoform in renal cells is not as well characterized as that of Nox4.

Our in vitro data demonstrate that silybin decreases superoxide generation in cultured podocyte and the in vivo study showed a similar effect in the kidney cortex. These findings, together with previous reports of silybin-induced reduction of fibronectin accumulation by human mesangial cells exposed to HG (57) and of protection of the kidney from arsenic toxicity via a decrease in ROS generation and apoptosis of tubular cells (40), clearly support the concept that silybin targets several cell types involved in the pathogenesis of diabetic nephropathy. This is not surprising considering that oxidative stress and enhanced generation of ROS is the underlying mechanism of injury to multiple cell types. It is tempting to speculate that inhibition of Nox4 function may be the common protective mechanism of silybin in all these cell types, since it is also known that Nox4-derived ROS play a key role in glucose-mediated mesangial cell injury.

Contrary to what is observed in diabetic renal tissue where Nox4 promotes apoptosis, Nox-derived ROS are described as antiapoptotic in cancer cells (36, 53). Interestingly, in cancer cells, silybin exerts proapoptotic rather than antiapoptotic effects as seen in diabetes (12, 27, 51). Therefore, it appears that Nox-derived ROS and silybin effects on cell survival differ in normal vs. malignant cells. Given that Nox4 has been implicated in numerous cancers (4), it is possible that Nox4 constitutes a prominent target of silybin in cells. These findings emphasize the complexity of the interaction between therapeutic or toxic xenobiotics and the biological conditions under which oxidative stress occurs.

Besides the herein described effect of silybin on NADPH oxidase and superoxide production, several other antioxidant effects targeting a variety of cells and tissues have been attributed to this compound and/or analogs including direct scavenging of free radicals, inhibition of the formation of other unstable compounds besides superoxide (14, 54, 62), maintenance of glutathione and other endogenous antioxidant redox balance (31, 33), as well as enhanced expression of the antioxidant enzymes glutathione peroxidase, glutathione reductase, superoxide dismutase, and catalase (8, 38). Furthermore, silybin suppresses the production of inflammatory cytokines incriminated in the pathogenesis of diabetic nephropathy including tumor necrosis factor-α (2, 32, 52) and transforming growth factor-β_1 (25, 39, 47). The effects of silybin therefore may not be limited to inhibition of NADPH oxidase activity and to prevention of podocyte injury and loss, and they may be extended to protection against other renal and nonrenal complications of diabetes mellitus.

In conclusion, this study demonstrates a protective effect of the antioxidant silybin against HG-induced podocyte injury and extends this finding to an animal model of type 1 diabetes and diabetic nephropathy. Our data support the concept that silybin may represent a novel therapeutic intervention for the treatment of diabetic nephropathy. Clinical trial aiming to determine the efficacy of silybin-containing flavonoids (milk thistle) in diabetic nephropathy is currently underway (ClinicalTrials.gov No. NCT01265563).

GRANTS

This work was supported in part through National Center for Complementary and Alternative Medicine Grant AT-004490 (P. Fanti), Merit Review Grant 1I01CX000264 (P. Fanti), Juvenile Diabetes Research Foundation Multiproject Grants (Y. Gorin and H. E. Abboud), National Institute of Diabetes and Digestive and Kidney Diseases Grant RO1 DK 079996 (Y. Gorin), and American Physicians Fellowship for Medicine in Israel (K. Khazim).

DISCLOSURES

No conflicts of interest, financial or otherwise, are declared by the author(s).

AUTHOR CONTRIBUTIONS

Author contributions: K.K., Y.C.G., and R.C.C. performed experiments; K.K., Y.C.G., R.C.C., and P.F. analyzed data; K.K., Y.C.G., H.E.A., and P.F. interpreted results of experiments; K.K. and P.F. prepared figures; K.K. drafted manuscript; Y.C.G.,

H.E.A., and P.F. conception and design of research; H.E.A. and P.F. edited and revised manuscript; P.F. approved final version of manuscript.

REFERENCES

1. Atkins RC, Briganti EM, Lewis JB, Hunsicker LG, Braden G, Champion de Crespigny PJ, DeFerrari G, Drury P, Locatelli F, Wiegmann TB, Lewis EJ. Proteinuria reduction and progression to renal failure in patients with type 2 diabetes mellitus and overt nephropathy. Am J Kidney Dis 45: 281–287, 2005 [PubMed: 15685505]

2. Bannwart CF, Peracoli JC, Nakaira-Takahagi E, Peracoli MT. Inhibitory effect of silibinin on tumour necrosis factor-alpha and hydrogen peroxide production by human monocytes. Nat Prod Res 24: 1747–1757, 2010 [PubMed: 20981616]

3. Berhane AM, Weil EJ, Knowler WC, Nelson RG, Hanson RL. Albuminuria and estimated glomerular filtration rate as predictors of diabetic end-stage renal disease and death. Clin J Am Soc Nephrol 6: 2444–2451, 2011 [PMCID: PMC3186453] [PubMed: 21852671]

4. Block K, Gorin Y. Aiding and abetting roles of NOX oxidases in cellular transformation. Nat Rev Cancer 12: 627–637, 2012 [PMCID: PMC3711509] [PubMed: 22918415]

5. Bokemeyer C, Fels LM, Dunn T, Voigt W, Gaedeke J, Schmoll HJ, Stolte H, Lentzen H. Silibinin protects against cisplatin-induced nephrotoxicity without compromising cisplatin or ifosfamide anti-tumour activity. Br J Cancer 74: 2036–2041, 1996 [PMCID: PMC2074813] [PubMed: 8980410]

6. Cosentino F, Hishikawa K, Katusic ZS, Luscher TF. High glucose increases nitric oxide synthase expression and superoxide anion generation in human aortic endothelial cells. Circulation 96: 25–28, 1997 [PubMed: 9236411]

7. Cravedi P, Ruggenenti P, Remuzzi G. Proteinuria should be used as a surrogate in CKD. Nat Rev Nephrol 8: 301–306, 2012 [PubMed: 22391456]

8. Das SK, Mukherjee S. Biochemical and immunological basis of silymarin effect, a milk thistle (Silybum marianum) against ethanol-induced oxidative damage. Toxicol Mech Methods 22: 409–413, 2012 [PubMed: 22409310]

9. Dashti-Khavidaki S, Shahbazi F, Khalili H, Lessan-Pezeshki M. Potential renoprotective effects of silymarin against nephrotoxic drugs: a review of literature. J Pharm Pharm Sci 15: 112–123, 2012 [PubMed: 22365093]

10. Day RT, Cavaglieri RC, Feliers D. Apelin retards the progression of diabetic nephropathy. Am J Physiol Renal Physiol 304: F788–F800, 2013 [PMCID: PMC3602700] [PubMed: 23303408]

11. de Zeeuw D, Ramjit D, Zhang Z, Ribeiro AB, Kurokawa K, Lash JP, Chan J, Remuzzi G, Brenner BM, Shahinfar S. Renal risk and renoprotection among ethnic groups with type 2 diabetic nephropathy: a post hoc analysis of RENAAL. Kidney Int 69: 1675–1682, 2006 [PubMed: 16572114]

12. Deep G, Agarwal R. Chemopreventive efficacy of silymarin in skin and prostate cancer. Integr Cancer Ther 6: 130–145, 2007 [PubMed: 17548792]

13. Dehmlow C, Erhard J, de Groot H. Inhibition of Kupffer cell functions as an explanation for the hepatoprotective properties of silibinin. Hepatology 23: 749–754, 1996 [PubMed: 8666328]

14. Dehmlow C, Murawski N, de Groot H. Scavenging of reactive oxygen species and inhibition of arachidonic acid metabolism by silibinin in human cells. Life Sci 58: 1591–1600, 1996 [PubMed: 8649189]

15. Eid AA, Ford BM, Block K, Kasinath BS, Gorin Y, Ghosh-Choudhury G, Barnes JL, Abboud HE. AMP-activated protein kinase (AMPK) negatively regulates Nox4-dependent activation of p53 and epithelial cell apoptosis in diabetes. J Biol Chem 285: 37503–37512, 2010 [PMCID: PMC2988355] [PubMed: 20861022]

16. Eid AA, Gorin Y, Fagg BM, Maalouf R, Barnes JL, Block K, Abboud HE. Mechanisms of podocyte injury in diabetes: role of cytochrome P450 and NADPH oxidases. Diabetes 58: 1201–1211, 2009 [PMCID: PMC2671039] [PubMed: 19208908]

17. Fallahzadeh MK, Dormanesh B, Sagheb MM, Roozbeh J, Vessal G, Pakfetrat M, Daneshbod Y, Kamali-Sarvestani E, Lankarani KB. Effect of addition of silymarin to renin-angiotensin system inhibitors on proteinuria in type 2 diabetic patients with overt nephropathy: a randomized, double-blind, placebo-controlled trial. Am J Kidney Dis 60: 896–903, 2012 [PubMed: 22770926]

18. Forbes JM, Coughlan MT, Cooper ME. Oxidative stress as a major culprit in kidney disease in diabetes. Diabetes 57: 1446–1454, 2008 [PubMed: 18511445]

19. Gaedeke J, Fels LM, Bokemeyer C, Mengs U, Stolte H, Lentzen H. Cisplatin nephrotoxicity and protection by silibinin. Nephrol Dial Transplant 11: 55–62, 1996 [PubMed: 8649653]

20. Galluzzi L, Aaronson SA, Abrams J, Alnemri ES, Andrews DW, Baehrecke EH, Bazan NG, Blagosklonny MV, Blomgren K, Borner C, Bredesen DE, Brenner C, Castedo M, Cidlowski JA, Ciechanover A, Cohen GM, De Laurenzi V, De Maria R, Deshmukh M, Dynlacht BD, El-Deiry WS, Flavell RA, Fulda S, Garrido C, Golstein P, Gougeon ML, Green DR, Gronemeyer H, Hajnoczky G, Hardwick JM, Hengartner MO, Ichijo H, Jaattela M, Kepp O, Kimchi A, Klionsky DJ, Knight RA, Kornbluth S, Kumar S, Levine B, Lipton SA, Lugli E, Madeo F, Malomi W, Marine JC, Martin SJ, Medema JP, Mehlen P, Melino G, Moll UM, Morselli E, Nagata S, Nicholson DW, Nicotera P, Nunez G, Oren M, Penninger J, Pervaiz S, Peter ME, Piacentini M, Prehn JH, Puthalakath H, Rabinovich GA, Rizzuto R, Rodrigues CM, Rubinsztein DC, Rudel T, Scorrano L, Simon HU, Steller H, Tschopp J, Tsujimoto Y, Vandenabeele P, Vitale I, Vousden KH, Youle RJ, Yuan J, Zhivotovsky B, Kroemer G. Guidelines for the use and interpretation of assays for monitoring cell death in higher eukaryotes. Cell Death Differ 16: 1093–1107, 2009 [PMCID: PMC2757140] [PubMed: 19373242]

21. Gazak R, Walterova D, Kren V. Silybin and silymarin–new and emerging applications in medicine. Curr Med Chem 14: 315–338, 2007 [PubMed: 17305535]

22. Gorin Y, Block K, Hernandez J, Bhandari B, Wagner B, Barnes JL, Abboud HE. Nox4 NAD(P)H oxidase mediates hypertrophy and fibronectin expression in the diabetic kidney. J Biol Chem 280: 39616–39626, 2005 [PubMed: 16135519]

23. Gorin Y, Ricono JM, Kim NH, Bhandari B, Choudhury GG, Abboud HE. Nox4 mediates angiotensin II-induced activation of Akt/protein kinase B in mesangial cells. Am J Physiol Renal Physiol 285: F219–F229, 2003 [PubMed: 12842860]

24. Hwang J, Saha A, Boo YC, Sorescu GP, McNally JS, Holland SM, Dikalov S, Giddens DP, Griendling KK, Harrison DG, Jo H. Oscillatory shear stress stimulates endothelial production of O_2^- from p47phox-dependent NAD(P)H oxidases, leading to monocyte adhesion. J Biol Chem 278: 47291–47298, 2003 [PubMed: 12958309]

25. Jeong DH, Lee GP, Jeong WI, Do SH, Yang HJ, Yuan DW, Park HY, Kim KJ, Jeong KS. Alterations of mast cells and TGF-beta1 on the silymarin treatment for CCl(4)-induced hepatic fibrosis. World J Gastroenterol 11: 1141–1148, 2005 [PMCID: PMC4250703] [PubMed: 15754394]

26. Jim B, Ghanta M, Qipo A, Fan Y, Chuang PY, Cohen HW, Abadi M, Thomas DB, He JC. Dysregulated nephrin in diabetic nephropathy of type 2 diabetes: a cross sectional study. PLoS One 7: e36041, 2012 [PMCID: PMC3355157] [PubMed: 22615747]

27. Kauntz H, Bousserouel S, Gosse F, Raul F. Silibinin triggers apoptotic signaling pathways and autophagic survival response in human colon adenocarcinoma cells and their derived metastatic cells. Apoptosis 16: 1042–1053, 2011 [PubMed: 21779837]

28. Keane WF, Zhang Z, Lyle PA, Cooper ME, de Zeeuw D, Grunfeld JP, Lash JP, McGill JB, Mitch WE, Remuzzi G, Shahinfar S, Snapinn SM, Toto R, Brenner BM. Risk scores for predicting outcomes in patients with type 2 diabetes and nephropathy: the RENAAL study. Clin J Am Soc Nephrol 1: 761–767, 2006 [PubMed: 17699284]

29. Laurindo FR, Fernandes DC, Santos CX. Assessment of superoxide production and NADPH oxidase activity by HPLC analysis of dihydroethidium oxidation products. Methods Enzymol 441: 237–260, 2008 [PubMed: 18554538]

30. Li JJ, Kwak SJ, Jung DS, Kim JJ, Yoo TH, Ryu DR, Han SH, Choi HY, Lee JE, Moon SJ, Kim DK, Han DS, Kang SW. Podocyte biology in diabetic nephropathy. Kidney Int Suppl: S36–42, 2007

31. Loguercio C, Festi D. Silybin and the liver: from basic research to clinical practice. World J Gastroenterol 17: 2288–2301, 2011 [PMCID: PMC3098397] [PubMed: 21633595]

32. Lu P, Mamiya T, Lu LL, Mouri A, Niwa M, Hiramatsu M, Zou LB, Nagai T, Ikejima T, Nabeshima T. Silibinin attenuates amyloid beta(25–35) peptide-induced memory impairments: implication of inducible nitric-oxide synthase and tumor necrosis factor-alpha in mice. J Pharmacol Exp Ther 331: 319–326, 2009 [PubMed: 19638571]

33. Lu P, Mamiya T, Lu LL, Mouri A, Zou L, Nagai T, Hiramatsu M, Ikejima T, Nabeshima T. Silibinin prevents amyloid beta peptide-induced memory impairment and oxidative stress in mice. Br J Pharmacol 157: 1270–1277, 2009

[PMCID: PMC2743846] [PubMed: 19552690]

34. Menini S, Iacobini C, Oddi G, Ricci C, Simonelli P, Fallucca S, Grattarola M, Pugliese F, Pesce C, Pugliese G. Increased glomerular cell (podocyte) apoptosis in rats with streptozotocin-induced diabetes mellitus: role in the development of diabetic glomerular disease. Diabetologia 50: 2591–2599, 2007 [PubMed: 17901943]

35. Meyer TW, Bennett PH, Nelson RG. Podocyte number predicts long-term urinary albumin excretion in Pima Indians with Type II diabetes and microalbuminuria. Diabetologia 42: 1341–1344, 1999 [PubMed: 10550418]

36. Mochizuki T, Furuta S, Mitsushita J, Shang WH, Ito M, Yokoo Y, Yamaura M, Ishizone S, Nakayama J, Konagai A, Hirose K, Kiyosawa K, Kamata T. Inhibition of NADPH oxidase 4 activates apoptosis via the AKT/apoptosis signal-regulating kinase 1 pathway in pancreatic cancer PANC-1 cells. Oncogene 25: 3699–3707, 2006 [PubMed: 16532036]

37. Mundlos S, Pelletier J, Darveau A, Bachmann M, Winterpacht A, Zabel B. Nuclear localization of the protein encoded by the Wilms' tumor gene WT1 in embryonic and adult tissues. Development 119: 1329–1341, 1993 [PubMed: 8306891]

38. Muzes G, Deak G, Lang I, Nekam K, Gergely P, Feher J. Effect of the bioflavonoid silymarin on the in vitro activity and expression of superoxide dismutase (SOD) enzyme. Acta Physiol Hung 78: 3–9, 1991 [PubMed: 1763650]

39. Navarro-Gonzalez JF, Mora-Fernandez C. The role of inflammatory cytokines in diabetic nephropathy. J Am Soc Nephrol 19: 433–442, 2008 [PubMed: 18256353]

40. Nishikawa T, Edelstein D, Du XL, Yamagishi S, Matsumura T, Kaneda Y, Yorek MA, Beebe D, Oates PJ, Hammes HP, Giardino I, Brownlee M. Normalizing mitochondrial superoxide production blocks three pathways of hyperglycaemic damage. Nature 404: 787–790, 2000 [PubMed: 10783895]

41. Pagtalunan ME, Miller PL, Jumping-Eagle S, Nelson RG, Myers BD, Rennke HG, Coplon NS, Sun L, Meyer TW. Podocyte loss and progressive glomerular injury in type II diabetes. J Clin Invest 99: 342–348, 1997 [PMCID: PMC507802] [PubMed: 9006003]

42. Prabu SM, Muthumani M. Silibinin ameliorates arsenic induced nephrotoxicity by abrogation of oxidative stress, inflammation and apoptosis in rats. Mol Biol Rep 39: 11201–11216, 2012 [PubMed: 23070905]

43. Rasband WS. ImageJ. Bethesda, MD: National Institutes of Health, 1997–2012

44. Rossing K, Christensen PK, Hovind P, Parving HH. Remission of nephrotic-range albuminuria reduces risk of end-stage renal disease and improves survival in type 2 diabetic patients. Diabetologia 48: 2241–2247, 2005 [PubMed: 16170513]

45. Sedeek M, Callera G, Montezano A, Gutsol A, Heitz F, Szyndralewiez C, Page P, Kennedy CR, Burns KD, Touyz RM, Hebert RL. Critical role of Nox4-based NADPH oxidase in glucose-induced oxidative stress in the kidney: implications in type 2 diabetic nephropathy. Am J Physiol Renal Physiol 299: F1348–F1358, 2010 [PubMed: 20630933]

46. Shankland SJ, Pippin JW, Reiser J, Mundel P. Podocytes in culture: past, present, and future. Kidney Int 72: 26–36, 2007 [PubMed: 17457377]

47. Sharma K, McGowan TA. TGF-beta in diabetic kidney disease: role of novel signaling pathways. Cytokine Growth Factor Rev 11: 115–123, 2000 [PubMed: 10708959]

48. Steffes MW, Schmidt D, McCrery R, Basgen JM. Glomerular cell number in normal subjects and in type 1 diabetic patients. Kidney Int 59: 2104–2113, 2001 [PubMed: 11380812]

49. Su J, Li SJ, Chen ZH, Zeng CH, Zhou H, Li LS, Liu ZH. Evaluation of podocyte lesion in patients with diabetic nephropathy: Wilms' tumor-1 protein used as a podocyte marker. Diabetes Res Clin Pract 87: 167–175, 2010 [PubMed: 19969384]

50. Susztak K, Raff AC, Schiffer M, Bottinger EP. Glucose-induced reactive oxygen species cause apoptosis of podocytes and podocyte depletion at the onset of diabetic nephropathy. Diabetes 55: 225–233, 2006 [PubMed: 16380497]

51. Tiwari P, Kumar A, Balakrishnan S, Kushwaha HS, Mishra KP. Silibinin-induced apoptosis in MCF7 and T47D human breast carcinoma cells involves caspase-8 activation and mitochondrial pathway. Cancer Invest 29: 12–20, 2011 [PubMed: 21166494]

52. Toklu HZ, Tunali Akbay T, Velioglu-Ogunc A, Ercan F, Gedik N, Keyer-Uysal M, Sener G. Silymarin, the antioxidant component of Silybum marianum, prevents sepsis-induced acute lung and brain injury. J Surg Res 145: 214–222, 2008

[PubMed: 17950327]

53. Vaquero EC, Edderkaoui M, Pandol SJ, Gukovsky I, Gukovskaya AS. Reactive oxygen species produced by NAD(P)H oxidase inhibit apoptosis in pancreatic cancer cells. J Biol Chem 279: 34643–34654, 2004 [PubMed: 15155719]

54. Varga Z, Ujhelyi L, Kiss A, Balla J, Czompa A, Antus S. Effect of silybin on phorbol myristate actetate-induced protein kinase C translocation, NADPH oxidase activity and apoptosis in human neutrophils. Phytomedicine 11: 206–212, 2004 [PubMed: 15070174]

55. Vessal G, Akmali M, Najafi P, Moein MR, Sagheb MM. Silymarin and milk thistle extract may prevent the progression of diabetic nephropathy in streptozotocin-induced diabetic rats. Ren Fail 32: 733–739, 2010 [PubMed: 20540643]

56. Wang YK, Hong YJ, Huang ZQ. Protective effects of silybin on human umbilical vein endothelial cell injury induced by H_2O_2 in vitro. Vascul Pharmacol 43: 198–206, 2005 [PubMed: 16111923]

57. Wenzel S, Stolte H, Soose M. Effects of silibinin and antioxidants on high glucose-induced alterations of fibronectin turnover in human mesangial cell cultures. J Pharmacol Exp Therap 279: 1520–1526, 1996 [PubMed: 8968378]

58. West IC. Radicals and oxidative stress in diabetes. Diabet Med 17: 171–180, 2000 [PubMed: 10784220]

59. White KE, Bilous RW, Marshall SM, El Nahas M, Remuzzi G, Piras G, De Cosmo S, Viberti G. Podocyte number in normotensive type 1 diabetic patients with albuminuria. Diabetes 51: 3083–3089, 2002 [PubMed: 12351451]

60. Wolf G, Chen S, Ziyadeh FN. From the periphery of the glomerular capillary wall toward the center of disease: podocyte injury comes of age in diabetic nephropathy. Diabetes 54: 1626–1634, 2005 [PubMed: 15919782]

61. Wolf G, Ziyadeh FN. Cellular and molecular mechanisms of proteinuria in diabetic nephropathy. Nephron Physiol 106: p26–31, 2007 [PubMed: 17570945]

62. Wu CH, Huang SM, Yen GC. Silymarin: a novel antioxidant with antiglycation and antiinflammatory properties in vitro and in vivo. Antioxid Redox Signal 14: 353–366, 2010 [PubMed: 20578796]

63. Zheng S, Noonan WT, Metreveli NS, Coventry S, Kralik PM, Carlson EC, Epstein PN. Development of late-stage diabetic nephropathy in OVE26 diabetic mice. Diabetes 53: 3248–3257, 2004 [PubMed: 15561957]

Figures and Tables

Fig. 1.

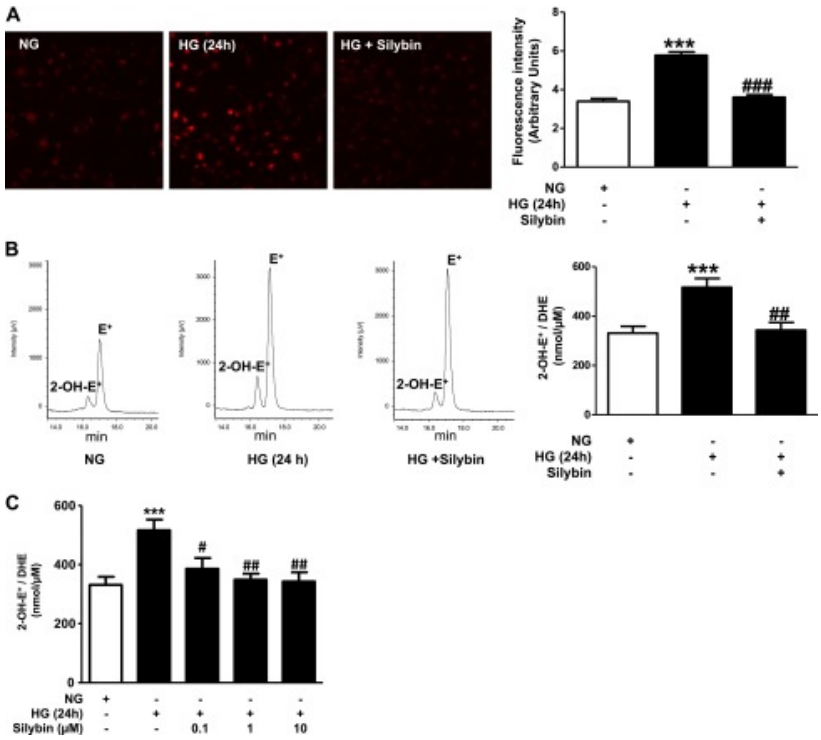

Silybin inhibits high glucose (HG)-induced superoxide generation. Exposure of mouse podocyte cultures to normal glucose (NG; 5 mM glucose) or to HG (25 mM glucose) with or without 10 μM silybin. Assessment of superoxide generation with the dihydroethidium (DHE) stain using 2 different methods: *A*, *left*: representative fluorescence microscopic images of podocytes after incubation with 10 μM DHE for 15 min. *A*, *right*: bar graph of semiquantitative analysis of the DHE fluorescence (means ± SE of 3 different experiments). ***$P < 0.0001$ HG vs. NG; ###$P < 0.0001$ HG vs. HG + silybin. *B*, *left*: representative HPLC elution profiles of the dihydroxyethidium (2-OH-E^+) peak, a DHE byproduct specific for superoxide generation, and the nonspecific ethidium (E^+) peak in cells extracts from cultured podocytes. *B*, *right*: bar graph of quantitative analysis of 2-OH-E^+ generation (means ± SE of 4 different experiments each experiment in triplicate). ***$P < 0.001$ HG vs. NG; ##$P <= 0.01$ HG vs. HG + 10 μM silybin. Results are expressed as nmol 2-OH-E^+/μM consumed DHE. *C*: dose-dependent response of cultured podocytes to silybin. Cells exposed to HG in the presence of 0.1, 1, or 10 μM silybin or vehicle. 2-OH-E^+ generation assessed by HPLC, as in *B* (***$P < 0.001$ HG vs. NG; #$P < 0.05$ HG vs. HG + 0.1 μM silybin; ##$P < 0.01$ HG vs. HG + 1 μM silybin; ##$P < 0.01$ HG vs. HG + 10 μM silybin).

Fig. 2.

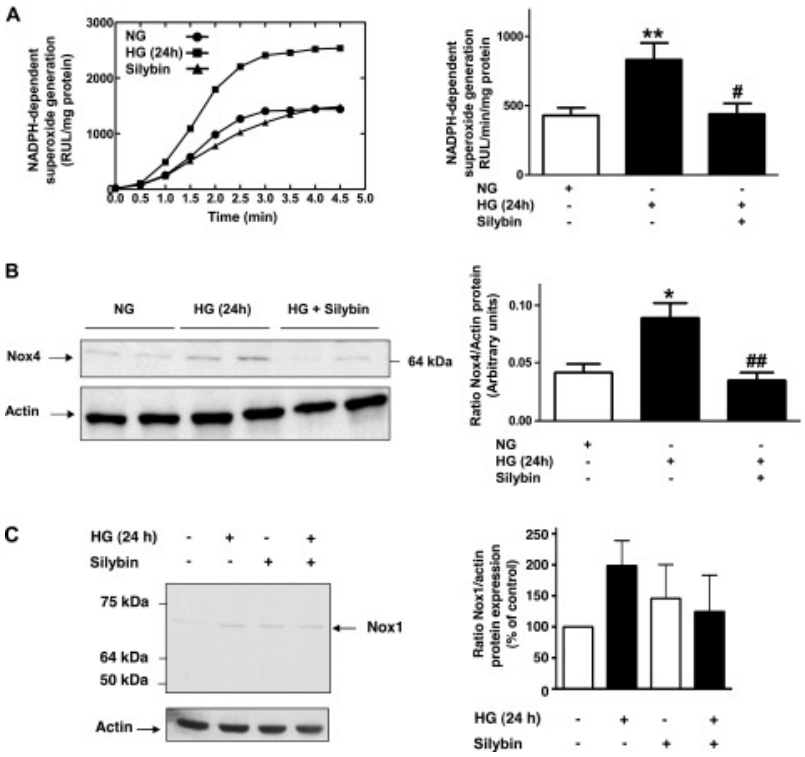

Effect of silybin on NADPH oxidase activity and Nox4 expression. Exposure of mouse podocytes to NG or HG without and with 10 μM silybin. *A*, *left*: representation of a representative individual experiment of NADPH-dependent superoxide generation in cultured cells, analyzed by lucigenin-enhanced chemiluminescence. Superoxide anion generation was determined by photoemission every 30 s for 4–5 min and was expressed as relative light units (RLU)/mg protein. *A*, *right*: bar graph of quantitative analysis of photoemission intensity expressed as $RLU \cdot min^{-1} \cdot mg\ protein^{-1}$ (means ± SE). $^{**}P < 0.01$ NG vs. HG; $^{\#}P < 0.05$ HG vs. HG + silybin. *B*, *left*: Western blotting analysis of Nox4 expression in homogenized podocytes. Actin was included as control for loading and for specificity of change in protein expression. *B*, *right*: bar graph of quantitative analysis of Nox4 densitometry corrected for actin band density (means ± SE; $^{*}P < 0.05$ NG vs. HG; $^{\#\#}P < 0.01$ HG vs. HG + silybin). *C*, *left*: representative Western blotting analysis of Nox1 expression in homogenized podocytes. Actin was included as control for loading and for specificity of change in protein expression. *C*, *right*: bar graph of quantitative analysis of Nox1 densitometry corrected for actin band density (means ± SE of 3 experiments).

Fig. 3.

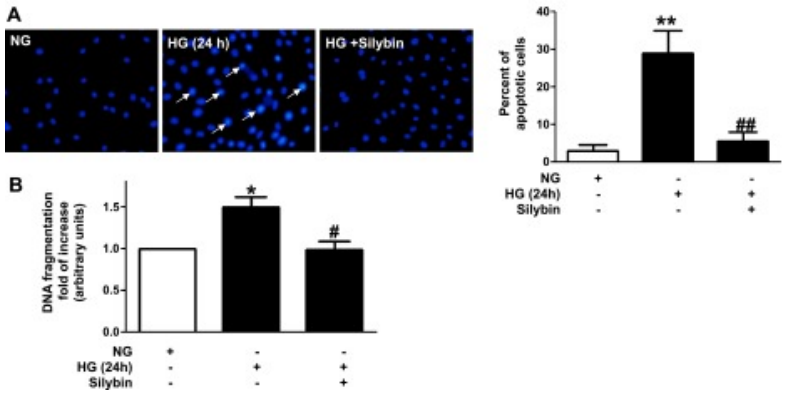

Effect of silybin on HG-induced podocyte apoptosis. Exposure of serum-deprived mouse podocytes to NG or HG for 24 h without or with 10 μM silybin. *A*, *left*: detection of apoptotic nuclei using Hoechst 33258. Chromatin condensation (white arrows) examined by fluorescent microscopy. *A*, *right*: bar graph of apoptotic cells as percent count of total cells (3 different experiments). $^{**}P < 0.01$ NG vs. HG; $^{\#\#}P < 0.01$ HG vs. HG + silybin. *B*: ELISA for cellular DNA fragmentation. Bar graph expresses the fold increase (means ± SE of 3 experiments in triplicate). $^{*}P < 0.05$ NG vs. HG; $^{\#}P < 0.05$ HG vs. HG + silybin.

Fig. 4.

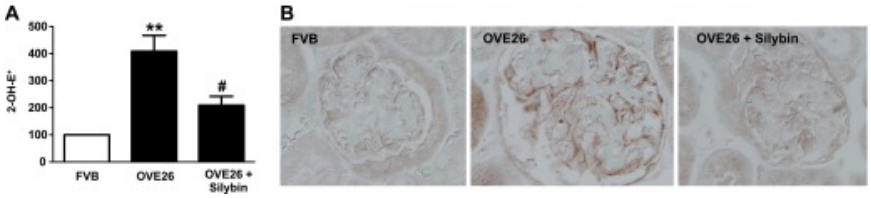

Silybin inhibits superoxide generation in diabetic mice kidney cortex and decreases the Nox4 protein expression. Measurement of superoxide generation in kidney cortex of 16-wk-old FVB mice, OVE26 mice, and OVE26 mice treated with silybin 100 mg/kg ip for 6 wk. *A*: bar graph of the percent increase in 2-OH-E^{+} generation in kidney cortex (means ± SE; $n = 4$ per group). $^{**}P < 0.01$ FVB vs. OVE26; $\#P < 0.05$ OVE26 vs. OVE26 + silybin. *B*: representative immunoperoxidase staining images of Nox4 protein in kidney sections from FVB (nondiabetic control), OVE26 (diabetic control), and OVE26 + silybin mice (diabetic treated).

Fig. 5.

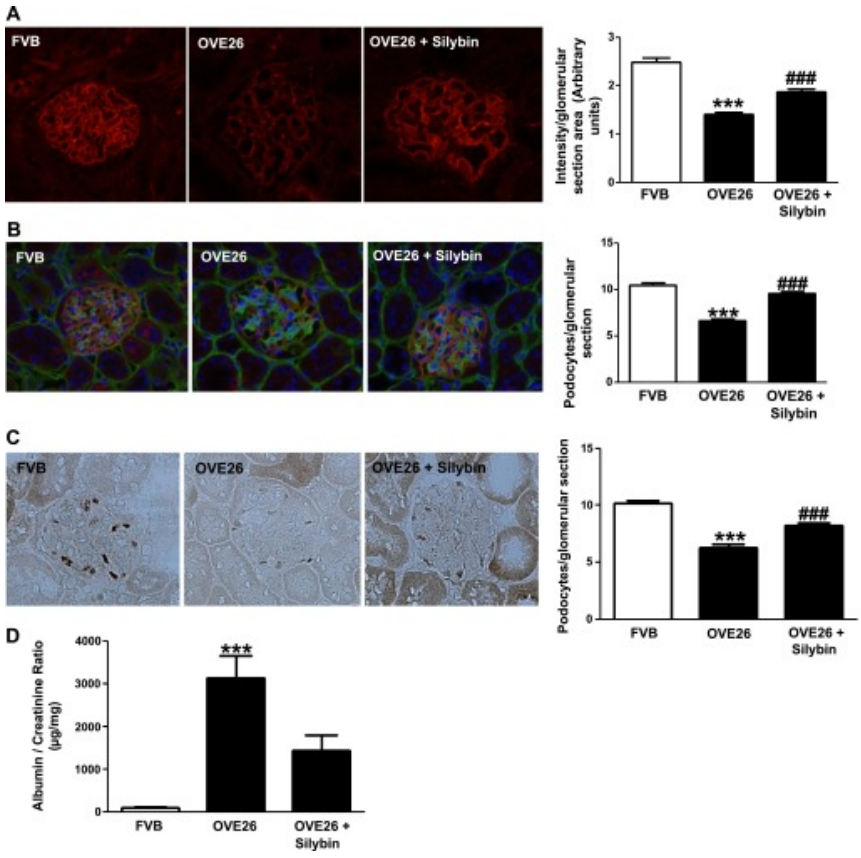

Silybin decrease podocyte injury in diabetic mice. *A*, *left*: representative immunofluorescence images of glomeruli stained for synaptopodin. *A*, *right*: bar graph of fluorescence intensity (means ± SE; $n = 3$ per group). ***$P < 0.001$ FVB vs. OVE26; ###$P < 0.001$ OVE26 vs. OVE26 + silybin. *B*, *left*: representative dual-label immunohistochemistry/fluorescence staining of glomeruli for podocyte count; basement membranes stained with collagen IV. *B*, *right*: bar graph of podocyte count per glomerulus (means ± SE; $n = 3$ per group). ***$P < 0.001$ FVB vs. OVE26; ###$P < 0.001$ OVE26 vs. OVE26 + silybin. *C*, *left*: representative immunoperoxidase staining of glomeruli for WT-1 protein expression. Right panel, bar graph of podocyte count per glomerulus (mean ± SE; $n = 3$ per group). ***$P < 0.001$ FVB vs. OVE26; ###$P < 0.001$ OVE26 vs. OVE26 + silybin. *D*: bar graph of albumin/creatinine ratio in 24-h urine samples from FVB, OVE26, and silybin-treated OVE26 mice. Urine collected over 24 h in metabolic cages after acclimatization. Albumin measured by ELISA and creatinine by colorimetry. Results expressed as µg protein/mg creatinine (means ± SE). ***$P < 0.001$ FVB vs. OVE26; $P = 0.06$ OVE26 vs. OVE26 + silybin.

Fig. 6.

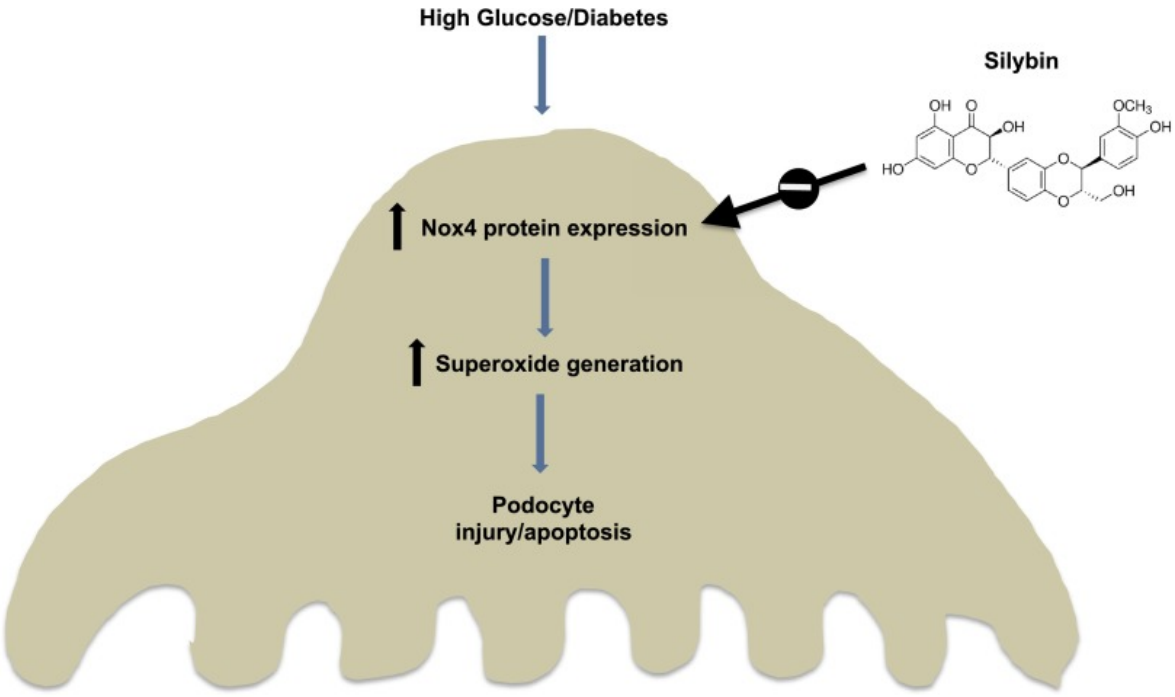

Proposed mechanism of the protective effect of silybin on HG/diabetes-induced podocyte injury/apoptosis.